Glucose Transporters and FDG Uptake in Untreated Primary Human Non-Small Cell Lung Cancer

Raya S. Brown, Jennifer Y. Leung, Paul V. Kison, Kenneth R. Zasadny, Andrew Flint and Richard L. Wahl

Division of Nuclear Medicine, Departments of Internal Medicine, Pathology and Radiology, The University of Michigan Medical Center, Ann Arbor, Michigan

PET imaging of malignant tumors with 2-[fluorine-18]-fluoro-2-deoxy-D-glucose (FDG) as a tracer is a noninvasive diagnostic and prognostic tool that measures tumor metabolism. In this study, we assessed the relationships between FDG uptake and the expression of facilitative glucose transporters, the sizes of populations of proliferating cells and infiltrating macrophages in patients with primary non-small cell lung cancers (NSCLC). **Methods:** FDG uptake and the expression of five glucose transporters and the proportions of proliferating cell and macrophage populations were studied in paraffin sections from untreated primary lung cancers by immunohistochemistry. The patients were imaged with FDG PET before surgery. **Results:** All tumors could be detected by FDG PET. Uptake was correlated with tumor size ($P = 0.004$). FDG uptake was lower in adenocarcinomas (ACs) than in squamous cell carcinomas (SQCs) ($P = 0.03$) or large cell carcinomas ($P = 0.002$) [standardized uptake value corrected for lean body mass (SUL) = 5.42 ± 2.77, 8.04 ± 3.25 and 10.42 ± 4.54, respectively]. Glut-1 expression was significantly higher than that of any other transporter. All tumors tested (n = 23) were Glut-1–positive (70.8% ± 26.1% of tumor cell area was positive and staining intensity was 2.8 ± 1.2). Glut-1 expression was higher in SQCs (78% ± 17.8% and 3.5 ± 0.6) than in ACs (47.5% ± 30.3% and 1.6 ± 1.1; $P = 0.044$ for positive tumor cell area and $P = 0.005$ for staining intensity). Proliferating cells constituted 15.3% ± 13.1% of the cancer cells, and the average number of macrophages was 7.8% ± 6.3%; neither correlated with FDG uptake. **Conclusion:** In this population of patients with NSCLC, Glut-1 is the major glucose transporter expressed. Both FDG uptake and Glut-1 expression appear to be associated with tumor size. No association was found between FDG uptake and either macrophage or proliferative cell populations.

Key Words: glucose transporters; human lung cancer; immunohistochemistry; FDG uptake

J Nucl Med 1999; 40:556–565

The high metabolism and increased rates of glucose consumption of cancers are associated with changes in the levels and isoenzyme compositions of glycolytic enzymes (*1–3*) and the overexpression of glucose transporters (*4–6*) compared with the surrounding normal tissues. Changes in the rates of glucose uptake and overexpression of glucose transporters are also associated with adaptation to hypoxia partly due to increased dependency on glycolysis as an energy source (*4,7*), a condition that may arise in rapidly growing tumors (*8*). These changes in glucose metabolism have been successfully used to diagnose, stage and monitor tumor response to therapy by (2-[fluorine-18]-fluoro-2-deoxy-D-glucose (FDG) PET imaging (*9*). It is currently accepted that increased influx of the glucose analog, higher rates of phosphorylation and diminished rates of dephosphorylation of the intracellular phosphorylated sugar are key factors in the cellular mechanisms underlying the high uptake and sequestration of FDG in cancer cells (*10*). Attempts to correlate the above-normal FDG uptake of tumors with their biological characteristics such as pathologic grade, proliferative activity or growth rate have not produced conclusive results (*11–14*). Similarly, contradictory results were obtained in studies evaluating the significance of FDG uptake by noncancerous components of the tumors to the overall uptake, although these nonmalignant components can be highly FDG avid (*15–17*). We observed a positive and significant correlation between FDG uptake and the number of viable cancer cells both in human cancer cell lines in vitro and in animal tumor studies in vivo (*15,18*).

To begin to evaluate the relationships between FDG uptake in human lung cancers, as assessed by PET, and the expression of glucose transporters, the sizes of the proliferating cell fraction or the macrophage population, we studied these parameters in patients with newly diagnosed non-small cell lung cancer (NSCLC) who were participating in a prospective study evaluating the use of PET for mediastinal staging of newly diagnosed primary lung tumors. The levels and extent of the expression of Glut-1, Glut-2, Glut-3, Glut-4 and Glut-5 glucose transporters in the untreated primary tumors were estimated in immunostained tissue samples with the polyclonal antibodies to the carboxy termini of each of these transporters. Sequential sections were immunostained with antiproliferating cell nuclear

Received Apr. 3, 1998; revision accepted Jul. 8, 1998.

For correspondence or reprints contact: Richard L. Wahl, MD, Division of Nuclear Medicine, University of Michigan Medical Center, 1500 E. Medical Center Dr., B1G 412, Ann Arbor, MI 48109–0028.

antigen (PCNA), a marker of proliferation, to identify cycling cells or with anti-CD68, a marker of human macrophages, to identify intratumoral macrophages. Standardized uptake values, corrected for lean body mass (SUL) (*19*), were calculated from the FDG PET images of the patients that were obtained before surgery.

MATERIALS AND METHODS

Patients

Fifty-nine patients with newly diagnosed non-small cell lung cancer (38 men, 21 women; age range 46–85 y; mean age 65.9 y) were imaged with FDG PET as part of a study evaluating PET for staging mediastinal tumor involvement. Diagnoses were 25 patients with adenocarcinoma (AC), 17 with squamous cell carcinoma (SQC), 9 with large cell carcinoma (LCC), 5 with tumors of both AC and SQC components, 1 SQC/LCC and 1 each of AC and SQC with small cell component. Six patients (all men) were diabetic. Thirty-nine patients underwent surgery, and tissue samples of 23 patients were available to be studied immunohistochemically. The average time interval between PET and surgery was 15 ± 7 d (median 14 d, range 3–30 d). All patients provided written informed consent for PET scanning and to have their tumor tissues studied experimentally.

Imaging Procedure and Image Data Analysis

PET was performed with an ECAT 921/EXACT scanner (CTI, Knoxville, TN) in 20 patients (11 of the Glut-1–stained tissues) and with an ECAT 931/08 scanner (CTI) in the other 39 (12 of the Glut-1–stained tissues). The patients fasted for at least 4 h before undergoing PET. Scanning was performed as described (*19*). SUL was calculated from attenuation-corrected images in scans obtained 50–60 or 60–70 min postinjection, as described in detail previously (*19*). The maximal 16-pixel region of interest (SUL) and the maximal pixel (MSUL) in the same region were recorded. Prescanning glucose levels (after 4 h with no food intake) were normal in 53 patients (88.6 ± 15.6 mg/dL, range 52–122 mg/dL, median 90.0 mg/dL). In 6 patients, glucose levels were high (143–370 mg/dL). No patient took insulin before PET.

Antibodies

Expression of glucose transporters was studied with polyclonal rabbit antiglucose transporter antibodies reactive with the carboxy terminus of Glut-1 (brain/erythrocyte, diluted 1:500), Glut-2 (liver, diluted 1:500), Glut-3 (brain, 5 μg/mL), Glut-4 (muscle/fat, insulin-regulatable, diluted 1:250) or Glut-5 (jejunum, 5 μg/mL) (East Acres Biological, Southbridge, MA). Tissues from 6 patients (patients 14–19, Table 1) were stained with another anti–Glut-1 polyclonal antibody to the carboxy terminus of the transporter

TABLE 1
Expression of Glucose Transporters in Non-Small Cell Lung Cancer

Patient no.	Tumor histology	Differentiation status	Glut-1		Glut-4	Pre-PET blood glucose (mg/dL)	SUL‡	MSUL§
			% area*	Intensity†				
1	AC	W	100	3	No staining	95.0	6.81	8.21
2	AC	W	20	0.5	50% of cells positive	102.0	5.23	6.78
3	AC	M	15	1	Some positive cells	73.0	4.45	5.70
4	AC	P	50	1	No staining	91.0	2.75	4.80
5	AC	P	50	1	Supranuclear granules	90.0	14.38	17.45
6	AC	P	50	3	Cell membrane	105.0	4.98	5.73
7	SQC	W	100	3	Cytoplasmic granules	60.0	5.44	5.95
8	SQC	M	90	1	Supranuclear and apical	338.0	3.58	4.54
9	SQC	M	80	4	Few positive cells	101.0	7.03	10.20
10	SQC	M	80	4	No staining	99.0	8.65	9.74
11	SQC	P	60	3	Few positive cells	112.0	7.16	8.37
12	SQC	P	90	3	No staining	83.0	8.07	10.23
13	SQC	P	100	3	Cell membrane	103.0	9.86	11.09
14	SQC	NA	50	4	ND	83.0	5.61	6.61
15	SQC	M	80	4	ND	89.0	4.85	5.91
16	SQC	P	90	2	ND	101.0	7.92	9.00
17	SQC	NA	90	1	ND	151.0	6.06	6.81
18	SQC	W	50	4	ND	71.0	7.02	8.06
19	SQC	M	80	4	ND	95.0	5.64	6.48
20	LCC	P	90	2	No staining	91.0	9.54	10.57
21	LCC	A	100	3	No staining	96.0	3.42	4.14
22	LCC	A	100	3	Cytoplasmic granules	305.0	4.92	5.80
23	LCC	A	80	2	Supranuclear granules	99.0	12.09	13.62

*Each value represents the relative Glut-1–positive area in tissue section (average section area was 3.59 ± 1.98 cm^2; the median 3.00 cm^2; range 1.0–8.0 cm^2).

†Intensity of staining estimated as described in Materials and Methods section.

‡Standardized uptake value corrected for lean body mass (SUL) is hottest 16-pixel region of interest in image and is a dimensionless parameter.

§Maximum SUL (MSUL) is the value for the maximum pixel in the 16-pixel region of interest.

AC = adenocarcinoma; SQC = squamous cell carcinoma; LCC = large cell carcinoma.

(Chemicon International, Inc., Temecula, CA), and tissues from 8 patients were stained with both. Staining SQC (*3*) and LCC (*2*) tissues with this antibody at 1:2000 dilution was similar to that with the East Acres antibody at 1:500. The intensity of staining with the Chemicom antibody was lower in AC (*3*) tissues compared with that of East Acres antibody. Preincubation of the Chemicon antibody with the East Acres antigen (a 12 AA mer) or with a 13 AA mer identical to the Chemicon antigen (Alpha Diagnostic International, San Antonio, TX) abolished the staining.

Proliferating cells were identified by nuclear binding of a monoclonal mouse PCNA, PC10 (Dako Corporation, Carpinteria, CA). This monoclonal antibody recognizes a 36-kd proliferating cell nuclear antigen and reacts with nuclei of a wide range of normal and neoplastic cells (*20*). Macrophages were identified by binding KP1, a monoclonal antibody raised against the lysosomal fraction of human lung macrophages (Dako). This antibody recognizes the pan-macrophage CD68 antigen (a 110-kd glycoprotein) of cells of the monocyte/macrophage lineage (*21*).

Immunohistochemistry

Serial paraffin sections from tumor tissues processed for routine pathology were immunostained for each of the glucose transporters, as described (*6,22*). Deparaffinized sections were incubated for 30 min in a 1:1 solution of 3% hydrogen peroxide and methanol to block endogenous peroxidase. Then, each consecutive tumor section was first incubated with antibodies to one of the peptide antigens for 1 h at room temperature. The binding sites were visualized by the avidin/biotin conjugate (ABC) immunoperoxidase procedure (*23*) using the Vectastain Elite kit (Vector, Burlingame, CA). Parallel sections incubated with normal rabbit IgG or with a mixture of the specific antibody and excess corresponding antigen (1:100) were used to verify the specificity of the staining (negative controls). Sections from paraffin-embedded brain (Glut-1–positive), liver (Glut-1– and Glut-2–positive), kidney (Glut-1–, Glut-2– and Glut-4–positive), pancreas (β-cells are Glut-2–positive), intestine (Glut-5–positive) and skeletal muscle (Glut-4–positive) from normal fasted rats were used as positive controls.

To identify PCNA-positive cells, additional parallel sections were incubated with PC10 diluted 1:50. Slides incubated with hybridoma medium or normal mouse IgG were used as negative controls, and paraffin sections of small intestine from a normal fasted rat were used as positive controls. To identify macrophages, slides were first digested with porcine trypsin solution, 1.25 g/L (Sigma, St. Louis, MO) to "unmask" binding sites and then incubated with 1:100 dilution of KP1. Sections incubated with normal mouse IgG were used as negative controls. Staining of alveolar macrophages present in the tumor-free lung area served as a positive control. All immunostained slides were lightly counterstained with hematoxylin and examined by light microscopy.

Estimates of Antigen-Positive Cells

Section sizes ranged from 1.0 to 8.0 cm^2 (average 3.6 ± 2.0 cm^2). Each section was divided into squares of 2 mm^2 area with the aid of a grid. Ten squares were randomly selected with the aid of a random numbers table and their locations on the section were marked. One 400× field at the upper right corner of the mark was counted. In each such field, the total number of cancer cells and the number of antigen-positive cells were counted. The average percentage of positive cells was calculated for 10 fields for each of the tumors.

Statistics

The equality of the histologic types was tested by the Mann-Whitney nonparametric two-sample test using the Statview PowerPC version. Pearson correlations were computed between FDG uptake and Glut-1 expression, percentage of proliferating cells, percentage of macrophages and tumor size. Data from the diabetic and nondiabetic patients were analyzed separately. Values are expressed as mean ± SD.

RESULTS

Expression of Glucose Transporters

Glut-1. All NSCLC tissues studied were Glut-1–positive (Table 1, Figs. 1a and 2a–c, 2f). In the nondiabetic patients (n = 20), 70.8% ± 26.1% (median 80.0%, range 15%–100%) of the cancer cell area was Glut-1–positive. The average intensity of staining was 2.8 ± 1.1 on a scale of 0 to 4. (In each section, staining intensity of red blood cells was referenced as intensity 4; median intensity was 3.0 [range 0.5–4]). Glut-1 staining was somewhat lower in the diabetic patients (n = 3, intensity of staining 2.0 ± 1.0, percentage of positive area 93.3% ± 5.7%). The intensity and extent of the expression of Glut-1 were significantly higher compared with Glut-4 (Fig. 1d) or the other transporters. The highest expression of Glut-1 was often observed in the membranes of the cancer cells (Figs. 1a and 2b and c) and in cancer cells around necrotic sites (Fig. 1a), but Glut-1–positive granules were also present throughout the cell cytoplasm. The expression of Glut-1 was considerably greater in the cell membranes of SQCs compared with ACs and LCCs (Figs. 2a–c and 3b and d). More positive cytoplasmic granules were observed in ACs and LCCs than in SQCs. In some ACs, clusters of Glut-1–positive granules were often seen in the supranuclear region of the cells. In these cells, no expression of the transporter was seen in the cell membrane (Figs. 2e and f).

No staining was observed in consecutive sections incubated with nonimmune serum (Fig. 1b) or with a mixture of the antibody and excess of Glut-1 antigen (results not shown). The overall staining intensities were higher and the proportions of positive areas were larger in SQCs than in ACs (P = 0.005 and 0.044, respectively [Table 2]). No immunohistochemically detectable Glut-1 was observed in the normal alveolar epithelium (Fig. 1f). Most of the macrophages found in the alveoli of adjacent tumor free lung were Glut-1–negative.

Glut-4. Eleven of 17 tumors stained were Glut-4–positive (Table 1). The expression of Glut-4 in NSCLC was much lower than that of Glut-1 and constituted less than 10% of the section's area. Glut-4–positive supranuclear granules were observed in 4 of 6 ACs (Fig. 2d). In one of these patients (patient 2), 50% of the tumor cells were Glut-4–positive (Fig. 1d). In this patient and in patient 5 (Table 1), the Glut-4–positive granules also appeared to be Glut-1–positive (Figs. 2e and f).

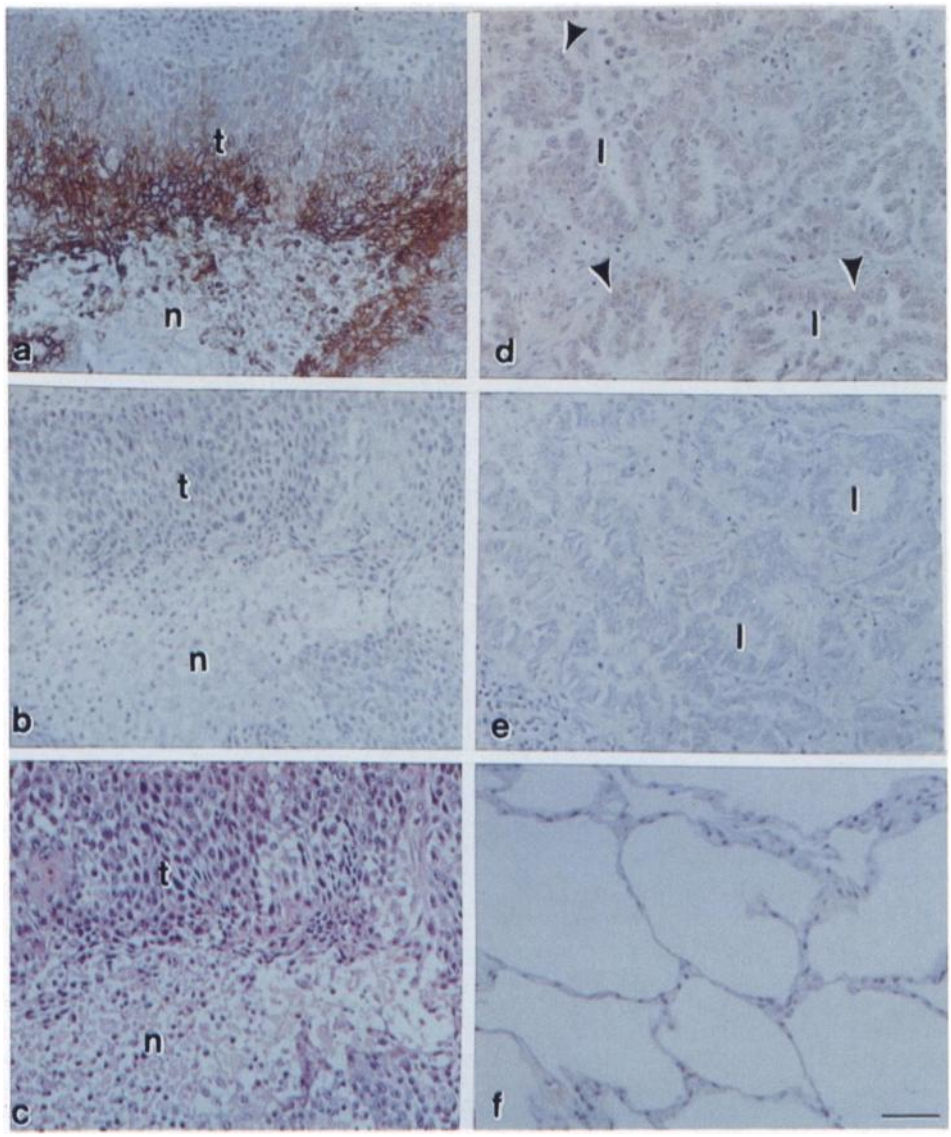

FIGURE 1. Expression of glucose transporters in NSCLC tissues. (a–c) Glut-1 expression in SQC (patient 10, Table 1). (a) High expression is seen near necrotic site (n). (b) Same area as in (a), immunostained with normal rabbit serum. (c) Same area as in (a), stained with hematoxylin and eosin. t = tumor cells. Note absence of inflammatory cells among cancer cells. (d–e) Glut-4 expression in AC (patient 2). (d) Glut-4–positive cytoplasmic granules (arrowheads) were seen in 50% of cancer cells. (e) Same area immunostained with mixture of anti–Glut-4 and antigen [Glut-4 carboxy terminus, a synthetic 12-mer peptide (CTELEYLGPEND)]. No staining is seen. (f) No staining of alveolar epithelium is seen in tumor-free area (patient 2). Magnification = ×125; bar = 50 μmol/L.

Sections incubated with nonimmune rabbit serum were not stained. Rat skeletal muscle fibers were Glut-4–positive but Glut-1–negative. Incubation with a mixture of anti–Glut-4 antibody with its antigen abolished the staining both in the tumor (Fig. 1e) and the rat muscle.

Glut-2, Glut-3 and Glut-5. Incubating with anti–Glut-2 resulted in a generalized faint and diffuse staining of the cytoplasm of the cancer cells. However, some strongly positive tumor cells were observed in 9 of the tumors (results not shown). All tumors were Glut-3–negative, but in 3 of the tumors some infiltrating leukocytes were Glut-3–positive. No staining of leukocytes was observed in sections incubated with normal rabbit IgG. None of the tumors expressed histochemically detectable Glut-5.

Proliferating Cells

Large variations in the numbers of PCNA-positive nuclei in different fields in the same tumor and between the different tumors were found (Fig. 4a). The percentage of PCNA-positive nuclei in cancer cells ranged from 0% to 38% (mean 15.8% ± 13.1%, median 18%) (Table 2). The differences between the 10 randomly chosen fields in the same tumor were also large. For example, the range for patient 3 was 7%–91% (mean 31% ± 26%), and for patient 21 it was 15%–48% (mean 33% ± 13%). In tissue samples from 6 patients, few PCNA-positive nuclei were observed throughout the tissue and they were considered negative. In 2 patients, about 1% of the cells were PCNA positive.

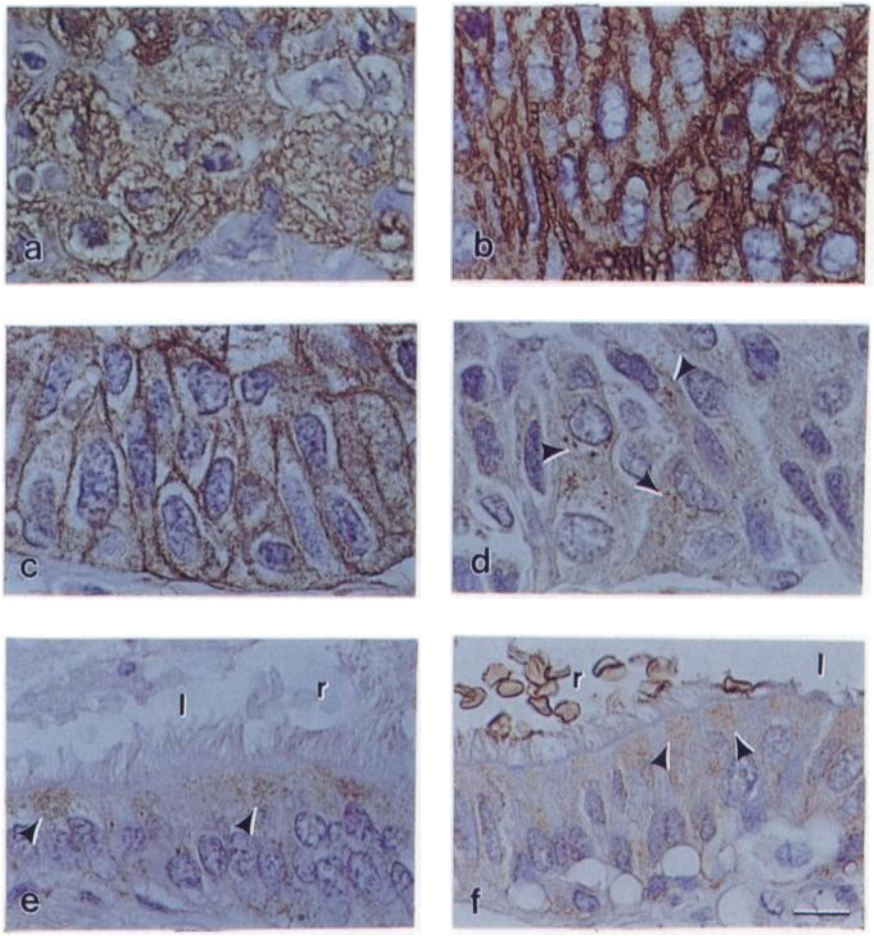

FIGURE 2. Patterns of staining in cancer cells in human lung cancers. (a) Glut-1 staining in LCC (patient 20). Same intensity of staining is seen in cytoplasmic granules and membranes of cancer cells. (b) Glut-1 staining in SQC (patient 11). Strong staining is seen in membranes of cancer cells. (c) Glut-1 staining in LCC (patient 22). High Glut-1 expression is seen in membrane, whereas intensity of staining of cytoplasmic granules is moderate. (d) Consecutive section of tissue from same patient as in (c) immunostained with anti–Glut-4. Cytoplasmic granules are Glut-4–positive, but there is no staining of cancer cell membranes. Clusters of strongly stained cytoplasmic granules are seen in some cells (arrowheads). (e) Glut-4 expression in proliferative bronchial epithelium inside tumor area from patient with AC (patient 4, Table 1). Note clusters of Glut-4–positive supranuclear granules. Note unstained red blood cells (r). l = lumen. (f) Glut-1 expression in same patient as in (e). Glut-1–positive granules are seen throughout cytoplasm. However, clusters of strongly stained supranuclear granules can also be seen (arrowheads). Note staining of red blood cells (r). Magnification = ×750; bar = 10 μmol/L.

CD68-Positive Cells

The number of CD68-positive cells varied considerably from field to field in the same tumor and between tumors (Figs. 4b–d). The average percentage of CD68-positive cells/tumor ranged from 0% to 22% (7.4% ± 6.4%) between tumors. The intratumoral range varied considerably. For example, it was 0%–73% in 1 patient (patient 5, AC, mean 10% ± 22%) whereas in another it was 0%–8% (patient 7, SQC, mean 1% ± 2%). In 5 of the patients, no intratumoral macrophages were found. There were fewer CD68-positive cells in SQCs than in either ACs or LCCs (Table 2). These differences were not statistically significant.

Tumor Sizes

Maximal and minimal tumor diameters estimated from pre-PET CT images were 4.2 ± 2.4 cm (median 4.0 cm) and 3.6 ± 2.3 cm (median 3.0 cm), respectively. The tumor sizes of the subpopulation of patients with stained tissues were similar to that of the subpopulation of patients with unstained tissues ($P = 0.39$ for maximal and $P = 0.15$ for minimal tumor diameters). Both maximal and minimal tumor diameters were smaller in ACs than in SQCs or LCCs (Table 3). The differences in both minimal and maximal diameters between the ACs and SQCs, but not between LCCs and the other pathological types, were statistically significant ($P = 0.033$ for maximal diameter and $P = 0.002$ for minimal diameter).

FDG Uptake

No significant correlation between FDG uptake and pre-PET blood glucose levels was found in these patients ($P = 0.26$ for SUL and $P = 0.28$ for MSUL). The SUL and MSUL were higher in the 53 nondiabetic patients than in the 6 diabetic patients (Table 3). No differences in FDG uptake were found between the subpopulation of patients with stained tissues and the subpopulation of patients with

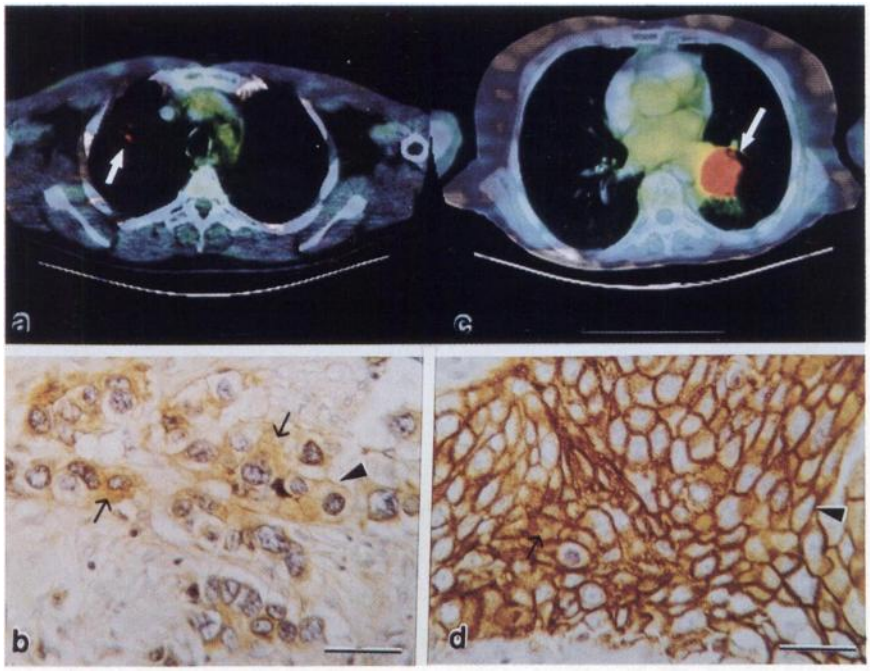

FIGURE 3. Fusion of PET and CT images of patient with AC (patient 3) and patient with SQC (patient 11). Fusion was accomplished using Mutual Information for Automatic Multimodality Image Fusion (MIAMI Fuse) software (*46*). For both cases a 9–control-point, thin plate spline warping was computed. (a) Fusion of PET and CT images of patient 3. Tumor diameter (arrow) was 3.0 cm, SUL was 4.45, MSUL was 5.7. (b) Glut-1 expression in patient 3. In this patient, 15% of cancer cells were Glut-1–positive, and staining intensity was 1. Note multiple cytoplasmic Glut-1–positive granules (arrow) and low binding to cell membrane (arrowhead). (c) Fusion of PET and CT images of patient 11. Tumor diameter (arrow) was 4.5 cm, SUL was 8.65, MSUL was 9.74. (d) Glut-1 expression in patient 11. In this patient, 80% of cancer cells were Glut-1–positive and staining intensity was 4. Note strong Glut-1 expression in cell membranes (arrowhead) and cytoplasmic Glut-1–positive granules (arrow) in some cells. Magnification = ×550; bar = 20 μmol/L.

unstained tissues (P = 0.90 for the SUL and 0.81 for the MSUL).

Significantly lower FDG uptake was found in ACs compared with LCCs for the whole patient population (n = 53) but not for the subpopulation of patients with stained tissues (n = 20) (Fig. 3, Table 3). Statistically significant correlations were found between FDG uptake and both maximal and minimal tumor diameters for the whole patient population (Table 3). Within histologic types, although FDG uptake increased with tumor size, the correlation was statistically significant for the ACs but not for the SQCs or LCCs (Table 4). No differences in either FDG uptake or tumor size were found between the nondiabetic subpopulations with stained tissues (n = 20) and with unstained tissues (n = 33). No statistically significant correlation was found between SUL or MSUL and either Glut-1 intensity, percent-

TABLE 2
Expression of Glut-1, Percentage PCNA Positive, Percentage CD68 Positive and FDG Uptake in Different Histological Types of Non-Small Cell Lung Cancers

Cancer	Glut-1–positive cells, % of tumor area	Intensity of staining (0–4)	Glut-1, intensity × % area	% PCNA positive nuclei in cancer cells*	% CD68-positive cells in tumor*	SUL	MSUL	n
All	70.8 ± 26.1	2.8 ± 1.2	215 ± 103	15.3 ± 13.3	7.8 ± 6.3	7.05 ± 2.86	8.43 ± 3.22	20
AC	47.5 ± 30.3†	1.6 ± 1.1‡	113 ± 111§	15.3 ± 12.9	10.3 ± 5.6	6.43 ± 4.11	8.11 ± 4.72	6
SQC	78.2 ± 17.8†	3.5 ± 0.6‡	272 ± 54§	15.7 ± 13.8	5.3 ± 6.8	7.02 ± 1.54	8.33 ± 1.87	11
LCC	90.0 ± 10.0	2.3 ± 0.5	213 ± 76	13.7 ± 17.2	11.0 ± 3.0	8.35 ± 4.46	9.44 ± 4.84	3

*Each value represents mean ± SD in 10 different fields/tumor. The average number of cells/400 × fields (0.8 mm²) was 165 ± 63 (median 165; range 74–294). These variations resulted from differences in the degree of reactive fibrosis and from presence or absence of lumens.

†The differences between the ACs and the SQCs in the % Glut-1–positive area are statistically significant (P = 0.044).

‡The differences between ACs and SQCs in the intensity of staining are statistically significant (P = 0.005).

§The differences between the ACs and the SQCs are statistically significant (P = 0.007).

SUL = standardized uptake value corrected for lean body mass; MSUL = maximal SUL; AC = adenocarcinoma, SQC = squamous cell carcinoma; LCC = large cell carcinoma.

Values given in mean ± SD.

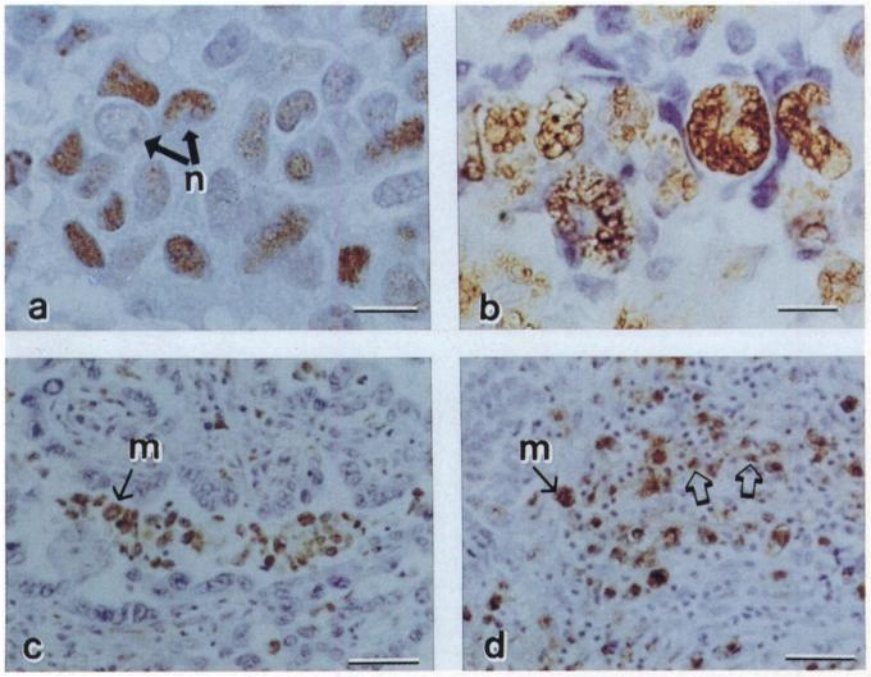

FIGURE 4. Expression of PCNA and CD68 in NSCLC tissues. (a) PCNA-positive nuclei in cancer cells in patient with AC (patient 4). Average number of PCNA-positive nuclei for this patient was 22 ± 18 (range 0%–52%). Magnification = ×700; bar = 10 μmol/L. (b) CD68-positive cells in tumor from same patient as in (a). Average number of CD68-positive cells for this patient was 9 ± 6 (range 3%–20%). Magnification = ×700; bar = 10 μmol/L. (c) CD68-positive cells in patient with AC. In this patient (patient 3), most of macrophages were observed in lumen. Average number of CD68-positive cells for this patient was 13 ± 3 (range 11%–19%). Magnification = ×240; bar = 50 μmol/L. (d) CD68-positive cells in patient with AC. Magnification = ×240; bar = 50 μmol/L. In this patient (patient 4), most macrophages and other infiltrating cells were observed in areas of cancer cells (arrows). l = lumen; m = macrophage; n = nucleus.

age of Glut-1–positive area, percentage of PCNA or percentage of CD68-positive cells.

DISCUSSION

These findings show that Glut-1, the mediator of basal glucose uptake in tissues, is the primary glucose transporter in human lung cancer and is expressed by most viable cancer cells. The contribution of the other transporters to the overall glucose metabolism in NSCLCs appears to be minor, as judged by their expression. The levels of expression or activity of Glut-1, or both, have been shown to be associated with transformation and malignancy and modified by changes in the physiological microenvironment in tissues (*4*,*7*,*24*). Moreover, it has been suggested that the cytokines and oncogene-induced upregulation of Glut-1–catalyzed glucose transport may have a role in the suppression of apoptosis, thus promoting leukaemogenesis (*25*). High Glut-1 expression coincides with increased metabolism and glucose utilization in several normal tissues (*26*,*27*), and the transporter is overexpressed in a variety of human tumors (*5*,*6*,*28*). Increased expression of Glut-1 is also seen in conditions that induce greater dependency on glycolysis as an energy source, such as ischemia, hypoxia or both (*29–31*). These data suggest that overexpression of Glut-1 may have an important role in the survival of cancer cells by promoting adequate energy supply to support their high metabolism and fast growth in an often less-than-ideal physiological environment (*32*).

In NSCLC, the extent and levels of Glut-1 expression and the intensely stained cell membranes are consistent with their high FDG uptake. The abundance and cellular localization of Glut-1, compared with other glucose transporters, suggest that Glut-1 may be the chief transporter for the movement of sugars into these cancer cells. The gradual increase in the expression of this transporter toward necrotic foci (Fig. 1a)—areas likely to have less-than-ideal blood flow and thus inadequate oxygenation (*8*,*33*)—indicate that intratumoral variations in Glut-1 expression may be affected by the levels of oxygen available to the cancer cells. The extensive binding of anti–Glut-1 to the cell membrane and the presence of Glut-1–positive cytoplasmic granules in the same cells may indicate that the cellular mechanism that regulates glucose (and FDG) uptake involves translocation of transporter from cytoplasmic reserves to the cell membrane.

Substantial differences in Glut-1 expression were found in NSCLC of different histologies. The expression of Glut-1 in SQCs was higher, and the proportions of positive areas were larger than in ACs. Moreover, in SQCs, the transporter tended to be primarily located on the cell membranes, which may indicate higher transport activity compared with ACs with numerous Glut-1–positive cytoplasmic granules and

TABLE 3
FDG Uptake in Non-Small Cell Lung Cancer Patients

	Nondiabetic	Diabetic	AC	SQC	LCC
SUL (all patients)	7.19 ± 3.79 (n = 53)	4.83 ± 1.61 (n = 6)	5.41 ± 2.78* (n = 25)	8.35 ± 3.25* (n = 16)	10.69 ± 4.47* (n = 6)
MSUL (all patients)	8.45 ± 4.29 (n = 53)	5.55 ± 1.75 (n = 6)	6.44 ± 4.21† (n = 25)	9.77 ± 3.77† (n = 16)	12.33 ± 5.39† (n = 6)
SUL (immunostained subpopulation)	7.05 ± 2.86 (n = 20)	5.0 ± 1.04 (n = 3)	6.43 ± 4.11 (n = 6)	7.02 ± 1.54 (n = 11)	8.35 ± 4.46 (n = 3)
MSUL (immunostained subpopulation)	8.43 ± 3.22 (n = 20)	5.72 ± 1.14 (n = 3)	8.11 ± 4.72 (n = 6)	8.33 ± 1.87 (n = 11)	9.44 ± 4.84 (n = 3)
Maximal tumor diameter (all patients)	4.2 ± 2.39 (n = 51)	5.4 ± 2.44 (n = 6)	3.61 ± 1.66‡ (n = 25)	4.61 ± 1.88‡ (n = 16)	6.38 ± 5.42‡ (n = 5)
Minimal tumor diameter (all patients)	3.58 ± 2.28 (n = 51)	4.82 ± 2.08 (n = 6)	2.65 ± 0.82§ (n = 25)	4.31 ± 1.79§ (n = 16)	5.56 ± 4.72§ (n = 5)
Maximal tumor diameter (immunostained subpopulation)	3.95 ± 1.66 (n = 20)	5.17 ± 2.84 (n = 3)	3.50 ± 1.46 (n = 6)	4.65 ± 1.37 (n = 11)	4.43 ± 2.71 (n = 3)
Minimal tumor diameter (immunostained subpopulation)	3.64 ± 1.57 (n = 20)	5.17 ± 2.84 (n = 3)	3.25 ± 1.57 (n = 6)	3.79 ± 1.28 (n = 11)	4.43 ± 2.71 (n = 3)

*Differences are statistically significant: for AC/SQC, $P = 0.015$; for AC/LCC, $P = 0.008$ but not for SQC/LCC.
†Differences are statistically significant: for AC/SQC, $P = 0.030$; for AC/LCC, $P = 0.014$ but not for SQC/LCC.
‡Differences are statistically significant for AC/SQC only; $P = 0.033$.
§Differences are statistically significant for AC/SQC only, $P = 0.002$.
AC = adenocarcinoma; SQC = squamous cell carcinoma; LCC = large cell carcinoma; SUL = FDG uptake in maximal 16-pixel region of interest corrected for lean body mass; MSUL = FDG uptake in the maximal 1 pixel in the same 16-pixel ROI corrected for lean body mass. Tumor diameters expressed in centimeters.

low membranous Glut-1 expression. On the basis of these data one may expect that FDG uptake will be lower in ACs compared with SQCs. Indeed, average FDG uptake calculated for all the nondiabetic patients was significantly lower in ACs than in SQCs or LCCs (Table 3). Although a similar pattern was observed in the immunostained subpopulation, the differences between the histologic types were not statistically significant. However, more tissues need to be evaluated to confirm these differences.

The expression of the insulin-regulatable glucose transporter, Glut-4, in NSCLC is much lower than that of Glut-1.

TABLE 4
Correlations between Tumor Size and FDG Uptake in Adenocarcinoma (AC) and Squamous Cell Carcinoma (SQC)

		SUL		MSUL	
	n	*r*	*P*	*r*	*P*
Maximal tumor diameter/all	52	0.40	0.004	0.35	0.011
Minimal tumor diameter/all	52	0.47	0.0004	0.44	0.012
Maximal tumor diameter/AC	25	0.48	0.015	0.40	0.045
Minimal tumor diameter/AC	25	0.72	<0.0001	0.68	0.0002
Maximal tumor diameter/SQC	16	0.37	0.20	0.30	0.081
Minimal tumor diameter/SQC	16	0.45	0.25	0.42	0.11

Data from diabetic patients are not included. There were 9 patients with large cell carcinoma; 3 were diabetics and no data of sizes were available for an additional patient. Therefore, correlations for this group are not presented.

The expression of Glut-4 is not unique to lung cancer and has been found in breast cancer and in several human gastrointestinal cancers (*6,34*). It is possible that Glut-4 may serve as an additional mechanism to ensure glucose influx into cancer cells because it may be regulated by mechanisms other than insulin, whether they may or may not be sensitive to insulin (*35*). It is conceivable that in some instances both transporters are induced either during carcinogenesis or as a response to specific physiological conditions, or both, in the microenvironment of the cancer cells. The presence and transport activity of both Glut-1 and Glut-4 in the same cells, as seen in some of these NSCLC tissues, have been reported in other tissues (*26*). Our finding that the two transporters co-localize in supranuclear granules in cells of ACs is consistent with the findings reported by Kraegen et al. (*26*) that intracellular Glut-4 vesicles of cardiac myocytes also contain a significant amount of Glut-1. However, the overall contribution of Glut-4 to hexose uptake in lung cancer, as judged by the level and extent of its expression in the tumors tested so far, is likely to be much smaller than that of Glut-1. The biological and clinical significance of the variations in Glut-4 expression in these tumors warrant additional studies.

In contrast to findings reported by Younes et al. (*36*), none of the NSCLC tissue we studied expressed Glut-3. This discrepancy could have resulted from the use of a different antibody or from differences in the size and characteristics of the patient populations studied, because 79% of the tumors they studied were Glut-3–negative and the percentage of Glut-3–positive cells in the positive tumors was low

compared to Glut-1. The presence of Glut-3-positive infiltrating inflammatory white cells in 3 of the tumors in this study is compatible with increased glucose metabolism in immune cells involved in host defense (*37*); this was also seen in human breast cancer (*6*) and in brain tissues (*38*). However, the number of the inflammatory cells in the tissues studied here constituted a small fraction of the tissue samples, therefore their contribution to the overall glucose uptake is probably not substantial.

The variations in the number of PCNA-positive cells among different fields of the same tumor or among tumors were very large. The percentages ranged from 0% to 73%, and the median was 15%, which is similar to those reported by Fontanini et al. (*39*), but averages (8%–20%) in this study were lower than the 52%–53% reported by Kawai et al. (*40*). However, these reports do not describe the method of selection of the fields to be counted; therefore, the possibility of bias in the selection of fields cannot be ruled out and the comparison may not be meaningful. There was no indication of any causal relationships between the size of the proliferating cell population and SUL or MSUL. This is consistent with the observation by Higashi et al. (*18*) that in vitro FDG uptake was correlated with the number of viable cells, but not with the proliferating cell fraction.

Variations in the number of macrophages in the same tumor and among tumors were large. Their numbers in SQCs were lower than in ACs or LCCs. However, FDG uptake in ACs was lower than that found in SQCs or LCCs. These findings suggest that the inflammatory cell component is not a major factor in FDG uptake in these primary lung cancers.

In the patients studied, FDG uptake as estimated by SUL or MSUL was strongly correlated with tumor size but not with Glut-1 expression. The latter does not necessarily contradict our previous results in an animal model in which we found a correlation between the intratumoral variations in tritiated FDG uptake and Glut-1 expression (*22*). It is possible that differences in transporter expression may determine the variations in FDG uptake at the cellular level, whereas intertumoral variations in FDG uptake at the whole tumor level may be determined by tumor blood flow and the rate of tracer delivery. Therefore the association between FDG uptake and Glut-1 expression at the whole tumor level is probably not as obvious as it is at the cellular level. On the other hand, tumor size, as well as both FDG uptake and Glut-1 expression, were significantly higher in SQCs than in ACs. It is conceivable that overexpression of Glut-1 may promote an increase in tumor size by supporting glycolytic metabolism that may not only enhance cancer cell viability but provide energy for cell division and tumor growth that results in larger tumors.

It cannot be ruled out that the differences in Glut-1 expression and FDG uptake between ACs and SQCs result from differences in their tumor biology and not from differences in tumor size. However, AC of the lung tends to metastasize and spread earlier than SQCs; therefore, it is possible that their size at presentation is smaller than those of SQCs. As a result, their Glut-1 expression and FDG uptake may be low. Although the correlation between FDG uptake and tumor size is statistically significant only for ACs, an increased FDG uptake with increased tumor size was also found for SQCs. The latter may indicate that in both histological types there is an association between tumor size and Glut-1 overexpression. The link between Glut-1 overexpression and transformation and carcinogenesis, as well the overexpression of this glucose transporter by many cancers, supports the view that overexpression of glucose transporters in cancer cells is biologically advantageous. It may ensure availability of metabolic intermediates for the biosynthetic pathways that are necessary for enhanced cell proliferation and tumor growth (*32,41*) as well as diminish the adverse effects of hypoxia in rapidly growing tumors.

Although these findings suggest some association between FDG uptake and Glut-1 expression, it is likely that the latter is not necessarily the sole or the rate-limiting step in this process. In addition to overexpression of Glut-1 and enhanced transport of glucose, many cancers have increased levels or activity of hexokinases, or both, as well as little, if any, glucose-6-phosphatase activity (*42*). It has been suggested that hexokinase lies at the core of the proliferative energy metabolism (*43*) and plays a critical role in initiating and maintaining the high glucose catabolic rates of rapidly growing tumors (*44*). Therefore, once FDG enters the cancer cells, hexokinase and glucose-6-phosphatase activities determine how much of the phosphorylated FDG is trapped in the cells. Indeed, Torizuka et al. (*45*) have suggested that phosphorylation, and not transport, is the limiting step in FDG uptake in breast cancer. However, in lung cancer, in vivo or in vitro, no correlation between phosphorylation and FDG uptake was found and the question of the relative importance of transport versus phosphorylation in this cancer is still unanswered.

CONCLUSION

These results suggest that (a) Glut-1 is the major glucose transporter expressed in NSCLC and is an important, although not the sole or rate-limiting, determinant in FDG uptake; (b) the pattern of tumor staining suggests that the transporter expression may be augmented by hypoxia; (c) the dual cellular localization of Glut-1, in the cell membranes and in cytoplasmic granules, may imply that the transport rate is partly regulated by translocation of Glut-1 from cytoplasmic reserves to the cell membrane; (d) Glut-4 may serve as an alternate or additional transporter; (e) the levels of both Glut-1 expression and FDG uptake are associated with tumor size; and (f) FDG uptake is not associated with the sizes of the intratumoral proliferative or the macrophage cell populations.

ACKNOWLEDGMENTS

We are grateful to Dr. Charles R. Meyer from the Department of Radiology, University of Michigan Medical

School, for his cooperation and help in using his Mutual Information for Automatic Multimodality Image Fusion (MIAMI Fuse) software. Supported by National Cancer Institute grant nos. CA 53172, CA 52880 and CA 56731.

REFERENCES

1. Warburg O, Posener K, Negelein E. The metabolism of the carcinoma cell. In: Warburg O, ed. *The Metabolism of Tumors.* New York, NY: Richard R. Smith, Inc.; 1931:129–169.
2. Weber G. Enzymology of cancer cells (first of two parts). *N Engl J Med.* 1977;296:486–492.
3. Golshani S. Insulin, growth factors, and cancer cell energy metabolism: an hypothesis on oncogene action. *Biochem Med Metab Biol.* 1992;47:108–115.
4. Merrall NW, Plevin R, Gould GW. Growth factors, mitogens, oncogenes and the regulation of glucose transport. *Cell Signal.* 1993;5:667–675.
5. Yamamoto T, Seino Y, Fukumoto H, et al. Over-expression of facilitative glucose transporter genes in human cancer. *Biochem Biophys Res Commun.* 1990;170:223–230.
6. Brown RS, Wahl RL. Overexpression of Glut-1 glucose transporter in human breast cancer. An immunohistochemical study. *Cancer.* 1993;72:2979–2985.
7. Ismail-Beigi F. Metabolic regulation of glucose transport. *J Membr Biol.* 1993;135:1–10.
8. Vaupel P, Kallinowski F, Okunieff P. Blood flow, oxygen and nutrient supply, and metabolic microenvironment of human tumors: a review. *Cancer Res.* 1989;49: 6449–6465.
9. Abdel-Dayem HM, Scott A, Macapinlac H, Larson S. Tracer imaging in lung cancer. *Eur J Nucl Med.* 1994;21:57–81.
10. Goldberg MA, Lee MJ, Fischman AJ, et al. Fluorodeoxyglucose PET of abdominal and pelvic neoplasms: potential role in oncologic imaging. *RadioGraphics.* 1993;13:1047–1062.
11. Di Chiro G, DeLaPaz RL, Brooks RA, et al. Glucose utilization of cerebral gliomas measured by [^{18}F] fluorodeoxyglucose and positron emission tomography. *Neurology.* 1982;32:1323–1329.
12. Minn H, Joensuu H, Ahonen A, Klemi P. Fluorodeoxyglucose imaging: a method to assess the proliferative activity of human cancer in vivo. Comparison with DNA flow cytometry in head and neck tumors. *Cancer.* 1988;61:1776–1781.
13. Haberkorn U, Strauss LG, Dimitrakopoulou A, et al. PET studies of fluorodeoxyglucose metabolism in patients with recurrent colorectal tumors receiving radiotherapy. *J Nucl Med.* 1991;32:1485–1490.
14. Strauss LG, Conti PS. The applications of PET in clinical oncology. *J Nucl Med.* 1991;32:623–648; [discussion] 649–650.
15. Brown RS, Leung JY, Fisher SJ, et al. Intratumoral distribution of tritiated fluorodeoxyglucose in breast carcinoma. I. Are inflammatory cells important? *J Nucl Med.* 1995;36:1854–1861.
16. Kubota R, Yamada S, Kubota K, et al. Intratumoral distribution of fluorine-18-fluorodeoxyglucose in vivo: high accumulation in macrophages and granulation tissues studied by microautoradiography. *J Nucl Med.* 1992;33:1972–1980.
17. Kubota R, Kubota K, Yamada S, et al. Active and passive mechanisms of [fluorine-18] fluorodeoxyglucose uptake by proliferating and prenecrotic cancer cells in vivo: a microautoradiographic study. *J Nucl Med.* 1994;35:1067–1075.
18. Higashi K, Clavo AC, Wahl RL. Does FDG uptake measure proliferative activity of human cancer cells? In vitro comparison with DNA flow cytometry and tritiated thymidine uptake. *J Nucl Med.* 1993;34:414–419.
19. Zasadny KR, Wahl RL. Standardized uptake values of normal tissues at PET with 2-[fluorine-18]-fluoro-2-deoxy-D-glucose: variations with body weight and a method for correction. *Radiology.* 1993;189:847–850.
20. Hall PA, Levison DA. Review: assessment of cell proliferation in histological material. *J Clin Pathol.* 1990;43:184–192.
21. Pulford KA, Sipos A, Cordell JL, Stross WP, Mason DY. Distribution of the CD68 macrophage/myeloid associated antigen. *Int Immunol.* 1990;2:973–980.
22. Brown RS, Leung JY, Fisher SJ, et al. Intratumoral distribution of tritiated fluorodeoxyglucose in breast carcinoma: correlation between Glut-1 expression and FDG uptake. *J Nucl Med.* 1996;37:1042–1047.
23. Hsu SM, Raine L, Fanger H. Use of avidin-biotin-peroxidase complex (ABC) in immunoperoxidase techniques: a comparison between ABC and unlabeled antibody (PAP) procedures. *J Histochem Cytochem.* 1981;29:577–580.
24. Mueckler M. Facilitative glucose transporters. *Eur J Biochem.* 1994;219:713–725.
25. Baldwin SA, Kan O, Whetton AD, et al. Regulation of the glucose transporter GLUT1 in mammalian cells. *Biochem Soc Trans.* 1994;22:814–817.
26. Kraegen EW, Sowden JA, Halstead MB, et al. Glucose transporters and in vivo glucose uptake in skeletal and cardiac muscle: fasting, insulin stimulation and immunoisolation studies of GLUT1 and GLUT4. *Biochem J.* 1993;295:287–293.
27. Camps M, Vilaro S, Testar X, Palacin M, Zorzano A. High and polarized expression of GLUT1 glucose transporters in epithelial cells from mammary gland: acute down-regulation of GLUT1 carriers by weaning. *Endocrinology.* 1994;134:924–934.
28. Younes M, Lechago LV, Somoano JR, Mosharaf M, Lechago J. Wide expression of the human erythrocyte glucose transporter Glut1 in human cancers. *Cancer Res.* 1996;56:1164–1167.
29. Kalff V, Schwaiger M, Nguyen N, McClanahan TB, Gallagher KP. The relationship between myocardial blood flow and glucose uptake in ischemic canine myocardium determined with fluorine-18-deoxyglucose. *J Nucl Med.* 1992;33:1346–1353.
30. Brosius FCI, Sun D, England R, Nguyen N, Schwaiger M. Altered glucose transporter mRNA levels in cardiac ischemia. *Circulation.* 1993;88:542A.
31. Clavo A, Brown R, Wahl R. 2-fluoro-2-deoxy-D-glucose (FDG) uptake into human cancer cell lines is increased by Hypoxia. *J Nucl Med.* 1995;36:1625–1632.
32. Newsholme EA, Board M. Application of metabolic-control logic to fuel utilization and its significance in tumor cells. *Adv Enzyme Regul.* 1991;31:225–246.
33. Graeber TG, Osmanian C, Jacks T, et al. Hypoxia-mediated selection of cells with diminished apoptotic potential in solid tumours. *Nature.* 1996;379:88–91.
34. Noguchi Y, Yoshikawa T, Doi C, et al. Expression of glucose transporters and insulin resistance in human GI cancer [abstract]. *Proc Annu Meet Am Assoc Cancer Res.* 1995;36:A1218.
35. Weinstein SP, O'Boyle E, Haber RS. Thyroid hormone increases basal and insulin-stimulated glucose transport in skeletal muscle. The role of GLUT4 glucose transporter expression. *Diabetes.* 1994;43:1185–1189.
36. Younes M, Brown RW, Stephenson M, Gondo M, Cagle PT. Overexpression of Glut1 and Glut3 in stage I non-small cell lung carcinoma is associated with poor survival. *Cancer.* 1997;80:1046–1051.
37. Peters JH, Hausen P. Effect of phytohemagglutinin on lymphocyte membrane transport. 2. Stimulation of "facilitated diffusion" of 3-O-methyl-glucose. *Eur J Biochem.* 1971;19:509–513.
38. Mantych GJ, James DE, Chung HD, Devaskar SU. Cellular localization and characterization of Glut 3 glucose transporter isoform in human brain. *Endocrinology.* 1992;131:1270–1278.
39. Fontanini G, Macchiarini P, Pepe S, et al. The expression of proliferating cell nuclear antigen in paraffin sections of peripheral, node-negative non-small cell lung cancer. *Cancer.* 1992;70:1520–1527.
40. Kawai T, Suzuki M, Kono S, et al. Proliferating cell nuclear antigen and Ki-67 in lung carcinoma. Correlation with DNA flow cytometric analysis. *Cancer.* 1994;74:2468–2475.
41. Warburg O. On the origin of cancer cells. *Science.* 1956;123:309–314.
42. Haberkorn U, Ziegler SI, Oberdorfer F, et al. FDG uptake, tumor proliferation and expression of glycolysis associated genes in animal tumor models. *Nucl Med Biol.* 1994;21:827–834.
43. Golshani-Hebroni SG, Bessman SP. Hexokinase binding to mitochondria: a basis for proliferative energy metabolism. *J Bioenerg Biomembr.* 1997;29:331–338.
44. Mathupala SP, Rempel A, Pedersen PL. Aberrant glycolytic metabolism of cancer cells: a remarkable coordination of genetic, transcriptional, post-translational, and mutational events that lead to a critical role for type II hexokinase. *J Bioenerg Biomembr.* 1997;29:339–343.
45. Torizuka T, Zasadny KR, Recker B, Wahl RL. Untreated primary lung and breast cancers: correlation between F-18 FDG kinetic rate constants and findings of in vitro studies. *Radiology.* 1998;207:767–774.
46. Meyer CR, Boes JL, Kim B, et al. Demonstration of accuracy and clinical versatility of mutual information for automatic multimodality image fusion using affine and thin-plate warped geometric deformations. *Med Image Analysis.* 1996/7;1:195–206.